



DESIGN CHARACTERIZATION OF SHAPE MEMORY ALLOY HELICAL STENT FOR ENDOHYPERThERMIA TREATMENT OF RESTENOSIS

A. Mahmood¹, F. A. Siddiqui², M.F. Hanif², A. Mahmood³, M.I. Malik⁴

¹Department of Mechanical Engineering, Tsinghua University, Beijing 100084, China

²Department of Mechanical Engineering, Bahauddin Zakariya University, Multan 60800, Pakistan

³Department of Electrical Engineering, COMSATS Institute of Information Technology, Pakistan

⁴Department of Electrical Engineering, Bahauddin Zakariya University, Multan 60800, Pakistan

Abstract

This paper proposes a helical type stent made by using Shape Memory Alloy (SMA) material, known as Nitinol. The stent is produced by laser cutting technique, having helical shaped zigzag loops in order to behave like an inductor. A capacitor is integrated on inductive stent to build an L-C tank circuit. This L-C resonant stent act as a wireless heater operated under Radio-Frequency (RF) magnetic field applied externally. The stent is fabricated by using 6 mm diameter Nitinol tubes with wall thickness of 0.1 mm having austenite finish (Af) temperature equals to 60°C. The helical stent is heated by applying potential difference across its ends and the results obtained from experiment were compared with the simulation results. It is concluded that the stent require 2.5 V or 1.5 Watts of energy to reach the temperature of 50° C which is an ideal temperature for hyperthermia treatment. The fabricated stent is electromechanically coupled with different types of capacitors in order to characterize its electrical properties and resonance frequency. The inductance of stent is found to be between 350 μ H – 400 μ H. At the end, mechanical properties of stent are also characterized and compared with commercial stent to ensure its practical validity.

Keywords: Shape Memory Alloy, LC Tank Circuit, Resonant Stent, Endohyperthermia

1. Introduction

Stents are broadly used to reopen partially blocked blood vessels and ducts of human body. Coronary artery stents are the most common type of stents to reduce blockage in coronary arteries followed by an invasive process known as Percutaneous Transluminal Coronary Angioplasty (PTCA) [1, 2]. More than 1.5 million patients with coronary artery blockage receive stent per year [3]. Although angioplasty is an effective treatment for partially blocked blood vessels, but restenosis or re-narrowing of blood vessels affect 30-40% of patients within 6 months, having a PTCA treatment [4]. Due to unsecure performance of existing stents, many new types of stents based on materials, techniques and designs have been proposed to improve the performance of stents in order to tackle restenosis. Drug Eluting Stents (DES) which release drugs such as Sirolimus and Paclitaxel offers a solution but has a risk of late stent thrombosis linked to it [5]. Other solution to restrain thrombosis is moderate heating of stents; somewhat around 50° C is effective to curb Thrombosis [6, 7].

* Corresponding Author: maw16@mails.tsinghua.edu.cn

A RF operated stent with appreciable results for hyperthermia treatment of restenosis is presented by [8]. These studies show satisfying results and provide a new direction in the development of stent.

Shape Memory Alloy (SMA), also known as Nitinol is famous about its actuation properties and biocompatibility [9, 10]. Self-expanding Nitinol stents are widely used for coronary artery implants [11]. Helical stent fabricated by laser cutting technique to serve as an inductor is proposed by [12], the stent structure show high inductance with a mechanically stable structure. The following stent is practically tested in vivo and delivered reliable results based on L-C tank stent technique in respective study [13]. Wireless MEMS devices taking advantage of L-C tank resonant circuits as wireless thermo-responsive micro-actuators utilizing SMA are reported in [14, 15]. In these mentioned studies, SMA micro-actuators were effectively actuated using external RF source with signals of strength less than 1W power.

In this paper a helical inductive stent is fabricated by laser cutting and its mechanical and electrical properties are characterized. Due to promising properties of SMA and its capability to operate wirelessly, an L-C resonant stent is build. A potential difference is applied to the stent to observe the heating characteristic of the stent in order to inhibit in-stent restenosis.

2. Design Principle

The active inductor-capacitor (L-C) stent is fabricated by laser cutting Nitinol tubes, behaves as a wireless actuator and heater. When L-C stent is exposed to RF magnetic flux, an AC current is spawned in the circuit which causes it to heat. To achieve maximum energy transfer the frequency of external RF sourced is tuned to match the resonance frequency of the L-C stent, which is $(2\pi^{-1}\sqrt{LC})$ and the system is operated at resonance condition. The power consumed in the LC circuit, P, can be expressed as [16]:

$$P(w) = \frac{Rv^2}{[R+j(\omega L-1/\omega C)]^2} \quad (1)$$

Where v is the electromotive force, L and C are inductance and capacitance of the circuit respectively, R is the parasitic resistance of the circuit and ω is the angular frequency of the AC current. The reactance in equation (1) is ousted when frequency of the AC current matches the resonance frequency of the circuit. At this condition maximum power can be transmitted to the circuit, which is:

$$P(\omega_r) = \frac{v^2}{R} \quad (2)$$

So, the field energy is adequately converted to Joule heat at resonance and the actuation can be controlled by tuning the frequency of external source. The steady state temperature rise of the LC circuit can be expressed as [17]:

$$T_{ss} = \frac{R_T v^2 / R}{1 + \alpha R_T v^2 / R} \quad (3)$$

Where R_T is the thermal resistance of the surrounding of circuit and αR is the temperature coefficient of resistance of the circuit. The resonance frequency of the stent device varies at its crimped and expanded state due to change in the inductance of stent at both conditions, shown in figure 1. The inductance of the stent can be found by:

$$L_s = \frac{\mu N^2 A}{l} \quad (4)$$

Where μ is the magnetic permeability of surrounding medium, N is the number of turns of solenoid/stent, l is the length, and A is the radial cross-sectional area of the stent.

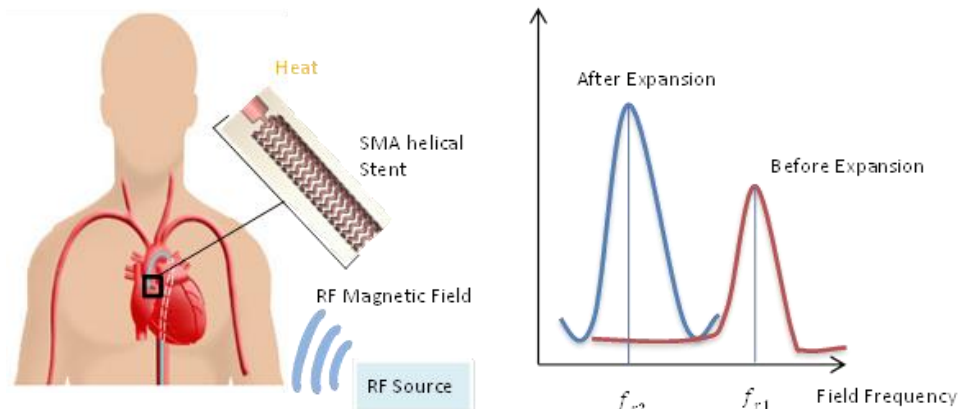


Figure 1: Conceptual illustration of L-C stent

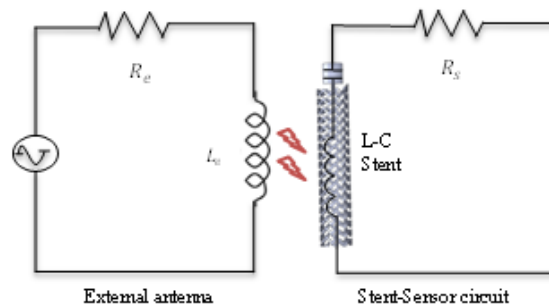


Figure 2: Equivalent circuit of L-C stent

As shown in figure 2, an external antenna is used to transfer RF magnetic power to the L-C stent. RF signal generator is attached to the external antenna and RF power similar to resonance frequency of the L-C stent is generated and transmitted to the stent. At this condition the L-C stent resonate and Joules heating phenomenon occur in the stent, which can help to heat the stent up to certain range of temperature depending on the frequency and strength of the RF signals.

3. Device Design and Fabrication

The stent is designed by keeping consideration of commercial stent dimensions and specifications in order to be implanted inside coronary artery by normal catheter system. A 3D model is first designed to observe the stent structure in 3D domain; the design is then transferred in to CAD model using AutoCAD 2013 software in order to be read by laser cutting equipment. The layout of stent is shown in figure 3. The stent structure is produced by using laser cutting equipment to cut 6 mm outer diameter Nitinol tubes with wall thickness of 0.1 mm. The actuation temperature (A_f) of Nitinol tube is 60°C . The stent is designed in such manner that its helical structure acts like an inductor and capacitor strips are cut out from the same tube and are fixed on the stent structure. The capacitor plates are bonded together with epoxy with 0.1 mm thick dielectric layer in between. The inductor capacitor L-C stent is electro polished after laser cutting and the final product is used for further investigation.

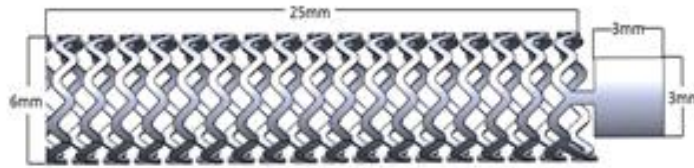


Figure 3: Layout of stent

This stent would work as a mechanical scaffold and an L-C tank circuit. Commercial stents normally have connection struts between the loops which cause electrical shortening and resulting in low inductance. A helical stent without having connection struts between the loops provides a stent of high inductance which aid to have an efficient L-C tank circuit. The helical stent contains 18 loops having 9 zigzag patterns in each loop. The length of stent is 25 mm with strut thickness of 335 μm ; these dimensions are chosen to have maximum inductance value. The capacitor strips are of 9 mm^2 area with 0.1mm polymer dielectric in between.

Stent fabricated from cylindrical Nitinol tubes is shown in figure 4. Dimensions of stent are as follows, length 25 mm, diameter 6 mm with strut width 335 μm .



Figure 4: Real stent

4. Experimental Setup and Results

In order to develop an L-C circuit that can be used as a wireless actuator and heater, the helical stent and a parallel plate capacitor are electromechanically coupled. The stent contains connecting pads at each of its ends, and these pads can be bonded to a parallel plate capacitor using conductive epoxy. Figure 4 shows the process flow for the fabrication of a parallel plate capacitor. The capacitor is fabricated by utilizing polyimide (PI) film of 100 μm thickness. First, a photoresist layer of thickness 2 μm is deposited on the PI film using AZ 1512 and baked at 95° C for 2 minutes. After this, a Ti/Au layer with thickness of 10 nm/50 nm is deposited on the PI film using an E-beam evaporator. The photoresist (PR) layer is removed by using acetone. Next, an SU-8 layer of 7 μm thickness is coated by a spinning coating process; it is first baked at 65° C and then at 95° C for 5 minutes each. After this, a second layer of Ti/Au having thickness of 10 nm/50 nm is deposited over the SU-8 layer to build a second parallel plate of the capacitor. At the end, a 7 μm thick SU-8 layer is deposited over the second capacitor strip in order to insulate the top surface of the capacitor.

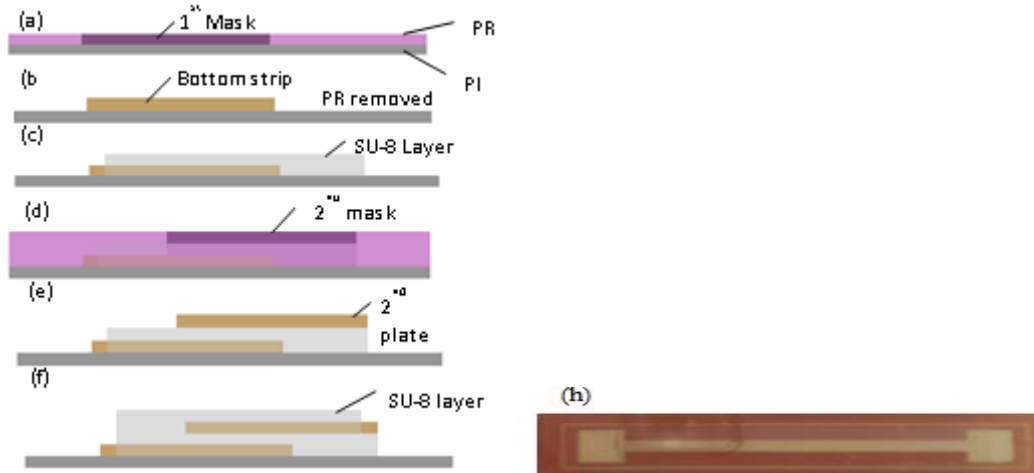


Figure 5: Process flow schematics of parallel plate capacitor (h) real device.

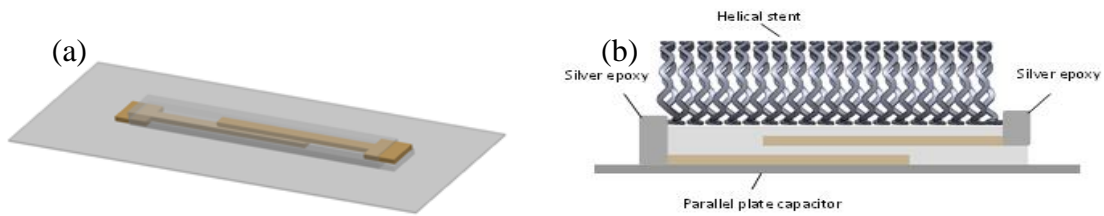


Figure 6 (a): 3-D view of fabricated parallel plate capacitor and (b) 3-D view of L-C stent

4.1. Resonance Frequency Measurement

Resonance frequency of fabricated L-C stent is measured by using Agilent 4395A spectrum-impedance analyser, through a wire interface established by bonding wire with the coil and directly coupled with the analyser. Figure 7 shows the types of stents used for impedance analysis and the result of L-C stent electromechanically coupled with different kinds of capacitors are obtained. Resonance frequency of number of devices is examined by using Agilent 4395A are listed in table 1.

Table 1: L-C pressure sensor data

Type of Stent	Sample # 1	Sample # 2	Sample # 3
Stent with commercial capacitor	$f_r=50.15 \text{ MHz}^*$ $f_r=51.25 \text{ MHz}^{**}$	$f_r=50.0 \text{ MHz}^*$ $f_r=52.50 \text{ MHz}^{**}$	$f_r=59.95 \text{ MHz}^*$ $f_r=57.5 \text{ MHz}^{**}$
Stent with Parallel Plate Capacitor	$f_r =182.5 \text{ MHz}^*$ $f_r =180.25 \text{ MHz}^{**}$	$f_r =134.5 \text{ MHz}^*$ $f_r =133.15 \text{ MHz}^{**}$	$f_r =180.9 \text{ MHz}^*$ $f_r =185.1 \text{ MHz}^{**}$
Stent with MEMS Capacitor	$f_r=52.32 \text{ MHz}^*$ $f_r=54.3 \text{ MHz}^{**}$	$f_r=54.5 \text{ MHz}^*$ $f_r=56.4 \text{ MHz}^{**}$	$f_r=53.25 \text{ MHz}^*$ $f_r=55.2 \text{ MHz}^{**}$
* Theoretically Calculated Value ** Practically Calculated Value			

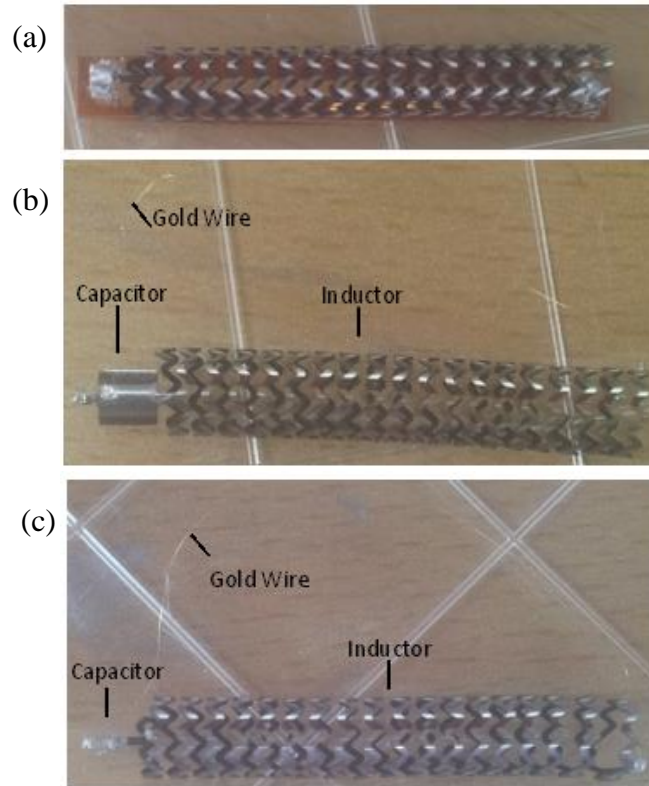


Figure 7 (a): L-C tank stent having parallel plate MEMS capacitor bonded by using silver epoxy (b) L-C tank stent having parallel plate capacitor bonded by non-conductive epoxy and (c) L-C tank stent with commercial capacitor

Resonance frequency measurement of different types of L-C stent shows that the theoretically calculated resonance frequencies of the stent match well with the experimentally measured values.

4.2. Joules Heating

A 2.5 V of applied voltage is applied across the ends of the L-C stent in order to observe the temperature distribution along its surface. The stent is heated due to joules heating phenomenon also known as resistive heating. It is evident that the temperature distribution is not uniform due to the non-uniform flux distribution along the surface of the stent. The stent has maximum temperature at the central region with a difference of around 15° C from the edges of the stent. The experimental results are verified using simulation on Comsole. The results of both simulation and experiment are in good agreement.

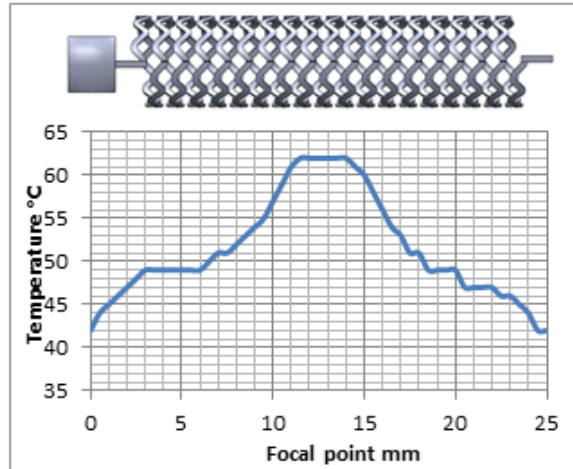


Figure 8: Temperature distribution along the stent surface at 3V of applied voltage

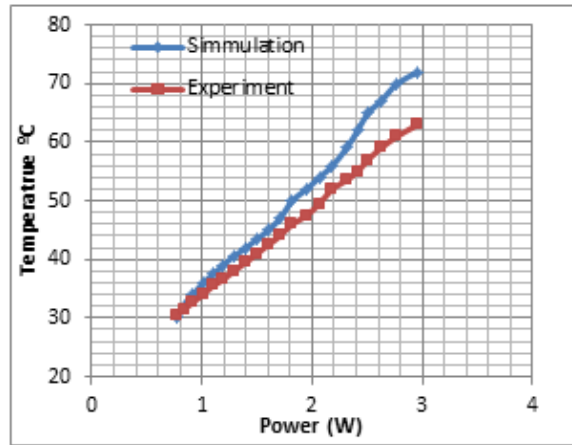


Figure 9: Average temperature on the stent surface as a function of applied power both experimental and simulation results



Figure 10: Temperature distribution along the stent surface at 3V of applied voltage, simulation result

Above results show that in order to heat the stent at around 50°C ; a 1.5 W of power would be required. This 1.5 W of power can be provided by using RF in order to heat the stent by non-invasive manner. The temperature distribution along the stent surface is not uniform and could cause complications while practical use. In future our aim is to improve the design parameters in order to have a uniform temperature distribution along the stent surface.

4.3. Mechanical Characterization

The radial-stiffness test results are plotted and shown in figure 11. It is evident from the results that the inductive stent is radially much stiffer than the commercial stent. As shown in the graph, in order to displace $2000\mu\text{m}$, the inductive stent required five times more force as compared to the commercial stent. The strut thickness of Nitinol stent in the helical stent was $300\mu\text{m}$ on average, and for $100\mu\text{m}$ for the commercial stent, three times higher than the commercial stent. Both stents had are made up of wire with approximately rectangular cross sections. Under the compression force, these wires experience a bending moment. As the overall radial stiffness of the stent is also dependent on its strut pattern, and which are different for both stents, this dimensional differences in the strut geometry is obviously the main cause of stiffness difference. In fact, higher radial stiffness of stent can be helpful to prevent failures of the device including recoil, which is one of the most common failure types for stents [18]; however this is directly proportional to the amount of metal with a stent that may increases the invasiveness of the device. Commercial stents available these days have a wide range of radial stiffness categories [19]. For the fabrication of inductive stent, radial stiffness of the final product can be controlled by utilizing electro- polishing, while maintaining the reliable thickness of the stent that has a greater influence on the stent's electrical performance as an inductor.

Figure 12 shows the results from the bending force analysis. As shown in the plots, 40mN force was required to be bent the commercial stent for $1500\mu\text{m}$ while only 20mN force was required for the helical stent to have $1500\mu\text{m}$ bending. It is evident that the ratio of bending force to displacement, i.e. the helical stent is two times more flexible than the commercial stent tested. The commercial stent is has low flexibility due to the presence of the links between the wire loops which prevent bending. It is also shown in the results that both stents showed highly elastic behaviours by returning to the points except the cobalt chrome stent because it show plastic characteristics after exceeding certain limit of force.

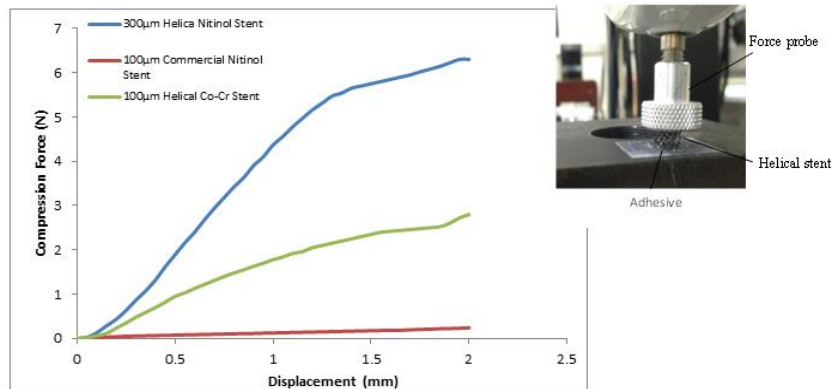


Figure 11: Measured radial forces as a function of displacement obtained with the inductive and commercial stent samples.

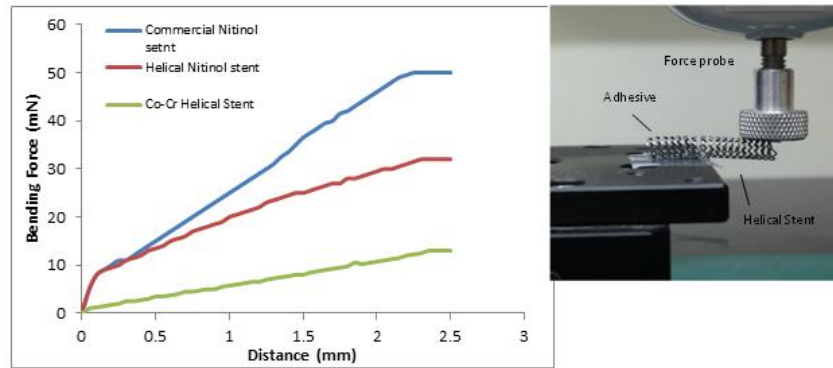


Figure 12: Comparison between bending compliances of inductive and commercial stents.

5. Conclusion

A new type of inductive stent using shape memory alloy is presented in this paper. The stent has a 25 mm long helical structure produced by laser machining of Nitinol tubes. Stent is heated by applying potential difference across its ends to observe the joules heating phenomenon and the results are compared with the simulation result. The stent can be effectively heated using external potential and can attain 50°C temperature with consumption of around 1.5 W. As the stent has to act as a mechanical scaffold, its mechanical properties are also verified and it is validated that stent can be effectively used for medical implants. The stent is also electromechanically coupled with different types of capacitors in order to check its electrical properties and capability to operate externally using RF source. It is evident that this stent can be effectively used as an RF heater for Endohyperthermia treatment. In future and external RF source would be utilised to heat the stent wirelessly.

References

- [1] R. Shepherd, F. J. Roger, R. E. Vlietstra, "The history of balloon angioplasty" Percutaneous transluminal coronary angioplasty, FA Davis Company, Philadelphia (1987): 1-17.
- [2] R. K. Myler, S. H. Stertzer, "Coronary and peripheral angioplasty: historical perspective." Textbook of interventional cardiology", WB Saunders 127 (1999): 41
- [3] E. P. McFadden, E. Stabile, E. Regar, E. Cheneau, A. T. Ong, T. Kinnaird, W. O. Suddath, N.J. Weissman, R. Torguson, K. M. Kent, A. D. Pichard, "Late thrombosis in drug-eluting coronary stents after discontinuation of antiplatelet therapy." The Lancet 364.9444 (2004): 1519-1521.
- [4] V. Rajagopal, S. G. Rockson, "Coronary restenosis: a review of mechanisms and management." The American journal of medicine 115.7 (2003): 547-553.
- [5] G. Mani, M. D. Feldman, D. Patel, C. M. Agrawal, "Coronary stents: a materials perspective." Biomaterials 28.9 (2007): 1689-1710.
- [6] C. Brasselet, E. Durand, F. Addad, F. Vitry, G. Chatellier, C. Demerens, M. Lemitre, R. Garnotel, D. Urbain, P. Bruneval, A. Lafont, "Effect of local heating on restenosis and in-stent neointimal hyperplasia in the atherosclerotic rabbit model: a dose- ranging study." European heart journal (2008)

- [7] C. J. Li, Y. F. Zheng, L. C. Zhao. "Heating NiTi stent in magnetic fields and the thermal effect on smooth muscle cells" *Key Engineering Materials* 288 (2005): 579-582.
- [8] Y. Luo, M. Dahmardeh, X. Chen, K. Takahata, "Selective RF heating of resonant stent toward wireless endohyperthermia for restenosis inhibition." *Micro Electro Mechanical Systems (MEMS), 2014 IEEE 27th International Conference on IEEE*, 2014
- [9] H. Kahn, M. A. Huff, A. .H. Heuer, "The TiNi shape-memory alloy and its applications for MEMS", *J. Micromech. Microeng.* 8 (1998) 213–221.
- [10] N. B. Morgan, "Medical shape memory alloy applications – the market and its products", *Mater. Sci. Eng A* 378 (2004) 16–23.
- [11] D. Stoeckel, A. Pelton, T. Duerig, "Self-expanding nitinol stents: material and design considerations." *European radiology* 14.2 (2004): 292-301.
- [12] A. R. Mohammadi, M. S. M. Ali, D. Lappin, C. Schlosser, K. Takahata, "Inductive antenna stent: design, fabrication and characterization." *Journal of Micromechanics and Microengineering* 23.2 (2013): 025015.
- [13] X. Chen, D. Brox, B. Assadsangabi, Y. Hsiang, K. Takahata, "Intelligent telemetric stent for wireless monitoring of intravascular pressure and its in vivo testing." *Biomedical microdevices* 16.5 (2014): 745-759.
- [14] M. S. M. Ali, B. Bycraft, A. Bsoul, K. Takahata, "Radio-Controlled Microactuator Based on Shape-Memory-Alloy Spiral-Coil Inductor" *Microelectromechanical Systems, Journal of* 22.2 (2013): 331-338.
- [15] M. S. M. Ali, K. Takahata, "Frequency-controlled wireless shape-memory-alloy microactuators integrated using an electroplating bonding process." *Sensors and Actuators A: Physical* 163.1 (2010): 363-372.
- [16] E. H. Sarraf, G. K. Wong, K. Takahata, "Frequency-selectable wireless actuation of hydrogel using micromachined resonant heaters toward implantable drug delivery application", in: *Proc. IEEE Transducers*, Denver, CO, USA, June 21–25, 2009, pp. 1525–1528.
- [17] S. D. Senturia, "Microsystem Design", Kluwer Academic Publishers, New York, 2001.
- [18] J. P. Carrozza, S. E. Hosley, D. J. Cohen, D. S. Baim, "In vivo assessment of stent expansion and recoil in normal porcine coronary arteries differential outcome by stent design." *Circulation* 100.7 (1999): 756-760.
- [19] R. Rieu, P. Barragan, C. Masson, J. Fuseri, V. Garitey, M. Silvestri, P. Roquebert, "Radial force of coronary stents: a comparative analysis. " *Catheterization and Cardiovascular Interventions* 46.3 (1999): 380-391.